International Journal of Academic Research and Development
www.allreviewjournal.com
ISSN: 2455-4197
Received: 05-05-2026, Accepted: 05-06-2026, Published: 20-06-2026
Volume 11, Issue 2, 2026, Page No. 97-106

# Phytochemical Profiling and alpha-amylase inhibitory potential of *Bauhinia monandra* extractives

**Yusuf Olalekan Barnabas**
Department of Chemistry, Federal College of Education, Okene, Kogi State, Nigeria
**DOI:** https://doi.org/10.66856/academic.2026.11.2.11058

**Abstract**
Diabetes mellitus continues to be a major non-communicable disease burden, particularly in sub-Saharan Africa, driving interest in plant-derived inhibitors of carbohydrate-metabolising enzymes. *Bauhinia monandra* Kurz (Fabaceae) is used across West Africa, India and tropical America in the traditional management of diabetes mellitus, yet the molecular basis of its activity against pancreatic alpha-amylase remains unresolved, and its flowers are essentially unstudied. This study profiled the phytochemistry of *B. monandra* leaf and flower and evaluated their alpha-amylase inhibitory potential. Air-dried leaf and flower material were separately extracted with ethanol and partitioned successively into n-hexane, dichloromethane, ethyl acetate, and aqueous fractions. Alpha-amylase inhibition was measured by the 3,5-dinitrosalicylic acid (DNSA) method with acarbose as the reference standard; total phenolic content (TPC) and total flavonoid content (TFC) were quantified; constituents were characterised by LC-MS and GC-MS; and identified compounds were docked against pancreatic alpha-amylase (PDB: 1HNY) using AutoDock Vina. The ethyl acetate fractions of both organs displayed the strongest, concentration-dependent inhibition, consistent with their highest phenolic and flavonoid contents. LC-MS identified quercetin, quercetin-3-O-rutinoside (rutin), quercetin-3-O-rhamnoside, and kaempferol derivatives, while GC-MS revealed beta-sitosterol, stigmasterol, and lupeol alongside fatty acid derivatives. Molecular docking positioned the identified flavonoids within the catalytic triad (Asp197, Glu233, Asp300) of alpha-amylase, with rutin and kaempferol achieving binding energies superior to acarbose. The results furnish the first integrated phytochemical and mechanistic rationale for the antidiabetic use of *B. monandra*, identify ethyl acetate-soluble flavonoids as the principal bioactive agents, and establish the flower as a credible source of alpha-amylase inhibitors.

**Keywords:** Bauhinia monandra, alpha-amylase, flavonoids, molecular docking, DNSA, antidiabetic, solvent partitioning, phytochemistry

## Introduction

Diabetes mellitus has become one of the defining non-communicable disease emergencies of the twenty-first century. The International Diabetes Federation (IDF) estimated that 537 million adults aged 20 to 79 years (a global prevalence of 10.5 percent) were living with diabetes in 2021 [14], a figure projected to rise to 643 million by 2030 and 783 million by 2045, representing a 46 percent increase that substantially outpaces population growth (Sun *et al*., 2022). More than 80 percent of this burden resides in low- and middle-income countries, and the disease was associated with more than 6.7 million deaths in 2021 alone (Sun *et al*., 2022). The World Health Organization separately attributed approximately 1.5 million deaths directly to diabetes in 2019, classifying it the ninth leading cause of death globally, with deaths rising roughly 70 percent between 2000 and 2019 (World Health Organization, 2021) [34]. Type 2 diabetes mellitus, which accounts for over 90 percent of all cases, is the dominant driver of this trajectory (International Diabetes Federation, 2021) [14].

In Nigeria, the problem is considerably more acute than international models suggest. A 2024 [22] systematic review and meta-analysis pooled the national type-2 prevalence at 7.0 percent (95% CI: 6.4 to 9.6%), translating to approximately 8.02 million affected adults, almost double the IDF-modelled estimate of 3.6 percent for the country (Olamoyegun *et al*., 2024) [22]. This disparity reflects the inadequacy of universal projection models for high-heterogeneity populations and underscores the need for locally anchored, cost-accessible therapeutic strategies. With most affected Nigerians unable to sustain long-term treatment with costly synthetic pharmaceuticals, the use of indigenous medicinal plants for diabetes management remains widespread and practically indispensable.

A central pathophysiological feature of type 2 diabetes is postprandial hyperglycaemia, driven by rapid enzymatic digestion of dietary starch. Pancreatic alpha-amylase (EC 3.2.1.1) initiates this process by cleaving internal alpha-1,4-glycosidic bonds to produce maltose and malto-oligosaccharides, which intestinal alpha-glucosidase subsequently converts to absorbable glucose (Brayer *et al*., 2000) [8]. Pharmacological inhibition of alpha-amylase attenuates this postprandial glucose surge, a strategy clinically validated by acarbose, miglitol, and voglibose. These agents, however, provoke dose-limiting gastrointestinal side effects, sustaining research interest in better-tolerated, plant-derived inhibitors (Kerru *et al*., 2018; Ogboye *et al*., 2021) [15, 20].

Structurally, human pancreatic alpha-amylase is a 57.6 kDa, 496-residue calcium metalloenzyme whose catalytic triad comprises Asp197 (nucleophile), Glu233, and Asp300 (acid/base catalysts), situated within an eight-stranded beta-barrel domain (Brayer *et al*., 2000) [8]. Mutation of Asp197 collapses enzymatic activity approximately one million-fold, underscoring the triad as the definitive pharmacological target for inhibitor design. Flavonoids have been shown to bind within or near this triad through hydrogen bonds with key residues, making them compelling

leads from plant sources (Proenca *et al*., 2022; Martinez-Gonzalez *et al*., 2019) [17, 25].

*Bauhinia monandra* Kurz (Fabaceae; Caesalpinioideae), the butterfly or orchid tree, known locally as *Abafe* among the Yoruba and as *casco de vaca* in Latin America, is employed in ethnomedicinal practice for diabetes management in Nigeria, Puerto Rico, and Brazil (Oshingboye, 2017; Menezes *et al*., 2007) [18, 24]. Pharmacological precedent for its antidiabetic action is substantial: a methanolic leaf extract at 2 g/kg reduced blood glucose by 65 percent in alloxan-diabetic rats, comparable to glibenclamide, and bioassay-guided fractionation identified quercetin and quercetin-3-O-rutinoside (rutin) as primary antihyperglycaemic constituents (Aderogba *et al*., 2006; Alade *et al*., 2012) [2, 4]. The stem bark has independently yielded antihyperglycaemic activity and lupeol-type triterpenes, methyl gallate, and beta-sitosterol (Ferrari *et al*., 2019) [11].

Despite this pharmacological precedent, three critical deficiencies persist. First, no study has linked *B. monandra* activity to alpha-amylase as a defined molecular target through the combined application of *in vitro* enzyme inhibition and in silico molecular docking. Second, the chemistry underpinning inhibition has not been simultaneously profiled by LC-MS and GC-MS within a single bioassay-guided partitioning framework. Third, the flower of *B. monandra*, which in related *Bauhinia* species is rich in anthocyanins and flavonoids, has been almost entirely ignored in the antidiabetic literature. This study addresses all three deficiencies.

## Literature Review

### 1. Global and Nigerian Diabetes Burden

The IDF Diabetes Atlas (10th Edition, 2021) [29] placed global diabetes prevalence at 537 million adults, with projections of 643 million by 2030 and 783 million by 2045 (Sun *et al*., 2022). Sub-Saharan Africa bears a disproportionate and rising share. The mortality burden is stark: Saeedi *et al*. (2020) attributed 4.2 million deaths to diabetes in 2019 [27] (11.3% of all-cause global mortality). In Nigeria, pooled national prevalence reached 7.0 percent (approximately 8.02 million adults), almost double earlier IDF projections, driven by urbanisation, physical inactivity, and dietary transition (Olamoyegun *et al*., 2024; Uloko *et al*., 2018) [22, 31].

### 2. Alpha-Amylase as a Therapeutic Target

Alpha-amylase catalyses the first step in starch digestion. Its catalytic triad (Asp197, Glu233, Asp300) is the definitive pharmacological target; substitution of Asp197 reduces activity approximately one million-fold (Brayer *et al*., 2000) [8]. Aromatic residues (Trp59, Tyr62, Tyr151) provide additional flavonoid contact points through hydrophobic stacking (Martinez-Gonzalez *et al*., 2019) [17]. Acarbose, the clinical reference inhibitor, achieves IC50 values of 23 to 77 micrograms per millilitre by DNSA assay; however, the DNSA method overestimates IC50 relative to chromogenic methods because acarbose is partially thermolabile under assay conditions (Visvanathan and Williamson, 2023) [33]. Among natural inhibitors, quercetin achieves IC50 of 0.325 mg/mL (versus acarbose 0.622 mg/mL), engaging the full catalytic triad non-competitively (Shen *et al*., 2023) [28], while rutin docks at -15.04 kcal/mol (AutoDock4, PDB 1OSE) versus acarbose -11.48 kcal/mol (Kulkarni and Kamble, 2021) [16].

### 3. Phytochemistry of *Bauhinia monandra* and Related Species

*Bauhinia monandra* phytochemistry is best characterised for the leaf and stem bark. Aderogba *et al*. (2006) [2] isolated quercetin-3-O-rutinoside and quercetin from the leaf; Alade *et al*. (2012) [4] confirmed these as the antihyperglycaemic constituents. Ferrari *et al*. (2019) [11] isolated lup-20(29)-en-3beta,24-diol, methyl gallate, and beta-sitosterol from the stem bark. Broader genus analysis has identified over 164 flavonoids in *Bauhinia*, including kaempferol, myricetin, quercetin, and their glycosides (Molecules, 2025) [19]. LC-MS studies on related species confirm myricetin ( [M-H]- m/z 317), quercetin (m/z 301), and kaempferol (m/z 285) as characteristic aglycones (Ye *et al*., 2012) [4]. GC-MS of Fabaceae members consistently reveals lupeol, beta-sitosterol, stigmasterol, phytol, squalene, and fatty acid derivatives.

### 4. Antidiabetic Activity of *Bauhinia monandra*

Alade *et al*. (2011) [5] demonstrated 65 percent blood glucose reduction at 2 g/kg in alloxan-diabetic rats, comparable to glibenclamide, with the butanol sub-fraction (BMBuF7) reducing hyperglycaemia by 43, 54, and 61.6 percent at one, two, and four hours respectively. Abo and Jimoh (2004) [1] confirmed antihyperglycaemic activity in the stem bark. Argolo *et al*. (2004) [1] established that chloroform and ethyl acetate extracts harboured the strongest antioxidant activity (IC50 approximately 2 mg/g DPPH). Campos *et al*. (2016) [9] documented anti-inflammatory and antinociceptive activities of the leaf lectin BmoLL. No prior study, however, has linked these effects to alpha-amylase inhibition or characterised the mechanistic interaction between constituent compounds and the enzyme active site.

### 5. Solvent Partitioning and Polarity-Dependent Bioactivity

Solvent partitioning concentrates flavonoid aglycones and glycosides in mid-polarity solvents, particularly ethyl acetate. Adesegun *et al*. (2019) [3] demonstrated the highest alpha-amylase inhibition (IC50 400 micrograms/mL) and phenolic/flavonoid content in the ethyl acetate fraction of *Sorindea warneckei*, attributed to concentrated quercetin, rutin, and gallic acid. Ojo *et al*. (2018) [21] reported ethyl acetate-fraction IC50 values of 24.04 and 25.11 micrograms/mL for alpha-amylase and alpha-glucosidase, respectively, in *Mangifera indica*. Similar patterns have been documented for *Salsola tetragona* and *Ficus lutea* (Olaokun and Zubair, 2023) [23]. Non-polar fractions consistently show lower phenolic content and weaker inhibition.

## Materials and Methods

### 1. Plant Collection and Authentication

Fresh leaves and flowers of *Bauhinia monandra* Kurz were collected in Okene metropolis, Kogi State, Nigeria (7.55 degrees N, 6.23 degrees E). The plant was authenticated by a plant taxonomist at the Herbarium Unit, Federal University of Technology, Minna, and a voucher specimen (FCE/OKN/CHE/2024/001) was deposited in the departmental herbarium. Collected material was rinsed, shade-dried at room temperature (27 to 32 degrees C) for three weeks to constant weight, milled to a coarse powder, and stored in amber-glass containers at 4 degrees C.

**2. Extraction and Solvent Partitioning**
Powdered leaf and flower (each 500 g) were separately macerated in 95 percent ethanol (1:10 w/v) for 72 hours with intermittent agitation and filtered through Whatman No. 1 paper; the marc was re-extracted twice. Combined filtrates were concentrated by rotary evaporation (Buchi R-210, 40 degrees C) to yield crude ethanol extracts. Each crude extract was suspended in 10 percent aqueous methanol and partitioned sequentially against n-hexane (3 x 200 mL), dichloromethane (3 x 200 mL), and ethyl acetate (3 x 200 mL), leaving an aqueous residue, yielding four fractions per organ (HF, DCM, EAF, AQF). All fractions were concentrated, weighed, and stored at 4 degrees C. This scheme follows the validated methodology of Ojo *et al.* (2018) [21].

**3. Qualitative Phytochemical Screening**
Standard phytochemical tests were applied for alkaloids (Mayer and Dragendorff reagents), flavonoids (Shinoda test), tannins (ferric chloride), saponins (froth test), phenolics, terpenoids and steroids (Salkowski and Liebermann-Burchard tests), cardiac glycosides (Keller-Kiliani test), and reducing sugars (Benedict's test) as described by Haruna and Yahaya (2021) [13]. Results were graded absent (-), trace (+), moderate (++), or abundant (+++).

**4. Total Phenolic and Flavonoid Contents**
TPC was determined by the Folin-Ciocalteu method (0.5 mL of 1 mg/mL solution + 2.5 mL 10% Folin reagent + 2 mL 7.5% Na2CO3; 37 degrees C, 30 min; absorbance at 765 nm) and expressed as mg GAE/g using a gallic acid calibration curve (R2 = 0.999). TFC was determined by aluminium chloride colorimetry (quercetin standard, R2 = 0.998) and expressed as mg QE/g. All analyses were conducted in triplicate.

**5. Alpha-Amylase Inhibition Assay (DNSA Method)**
Porcine pancreatic alpha-amylase (Sigma A3176; 0.5 mg/mL in 20 mM phosphate buffer pH 6.9, 6 mM NaCl) was pre-incubated (10 min, 37 degrees C) with extract/fraction solutions across eight concentrations (31.25 to 1000 micrograms/mL, triplicate). One millilitre of 1% (w/v) soluble starch was added and incubated (37 degrees C, 10 min); the reaction was stopped with 1.0 mL DNSA reagent, boiled 5 min, cooled, diluted with 10 mL distilled water, and absorbance read at 540 nm. Acarbose served as the positive control. Percentage inhibition was calculated as [(Acontrol - Asample)/Acontrol] x 100. IC50 values were derived by non-linear regression (GraphPad Prism 9). Results are expressed as mean +/- SD (n = 3). Because the DNSA method overestimates IC50 relative to chromogenic assays, results are interpreted comparatively across fractions rather than as absolute affinities (Visvanathan and Williamson, 2023) [33].

**6. LC-MS Analysis of Polar Fractions**
Ethyl acetate and aqueous fractions (1 mg/mL in methanol) were analysed by LC-ESI-MS (Agilent 6470 Triple Quadrupole) on a C18 reverse-phase column (Agilent Zorbax, 4.6 x 150 mm, 3.5 micrometre). Gradient: 0.1% formic acid in water (A) and 0.1% formic acid in acetonitrile (B); 0 to 5 min, 5% B; 5 to 35 min, 5 to 60% B; flow rate 0.5 mL/min. Negative-ion ESI mode (capillary 3.5 kV, drying gas 350 degrees C, 11 L/min, nebuliser 45 psi). Compounds were tentatively identified by [M-H]- ions and characteristic fragment ions against MassBank and MzCloud databases, using quercetin (m/z 301), kaempferol (m/z 285), rutin (m/z 609), and gallic acid (m/z 169) reference standards.

**7. GC-MS Analysis of Less-Polar Fractions**
n-Hexane and dichloromethane fractions (5 mg/mL in n-hexane) were analysed using a Shimadzu QP-2020 NX GC-MS with DB-5MS column (30 m x 0.25 mm x 0.25 micrometre). Temperature programme: 60 degrees C (2 min) to 280 degrees C at 5 degrees C/min; injector 280 degrees C; split 1:20; helium carrier gas at 1.0 mL/min; MS scan m/z 40 to 600 (EI, 70 eV). Compounds were identified by NIST 2020 library matching (minimum 80%) and confirmed by Kovats retention indices calculated against C8 to C40 n-alkane standards. Quantitative data are normalised peak area percentages.

**8. Molecular Docking**
Human pancreatic alpha-amylase (PDB: 1HNY, 1.8 Angstrom resolution; Brayer *et al*., 1995) [7] was retrieved from the RCSB PDB; water molecules and ligands were removed, polar hydrogens and Gasteiger charges added in AutoDock Tools 1.5.7. Ligand 3D structures (quercetin, rutin, kaempferol, beta-sitosterol, lupeol, acarbose) were retrieved from PubChem and energy-minimised (MMFF94, Avogadro). A grid box (30 x 30 x 30 Angstrom, 0.375 Angstrom spacing) was centred on Asp197/Glu233/Asp300. Docking used AutoDock Vina 1.2 (Trott and Olson, 2010) [30] with exhaustiveness 8 and nine output poses. Protocol validation: acarbose redocking yielded RMSD of 1.37 Angstrom relative to the crystal pose, confirming reliability. Interactions were visualised in UCSF Chimera and Discovery Studio Visualiser 2021.

**9. Statistical Analysis**
All *in vitro* data are expressed as mean +/- SD (n=3). One-way ANOVA with Tukey's HSD post-hoc test was applied for multiple-group comparisons; $p < 0.05$ was considered statistically significant. Pearson correlation coefficients were computed between TPC/TFC and IC50. Statistical analyses used IBM SPSS Statistics 26.0.

**Results**
**1. Extraction Yields and Qualitative Phytochemistry**
Ethanol extraction yielded 8.6% (w/w) from the leaf and 7.1% from the flower. Solvent partitioning produced the highest yield in the ethyl acetate fraction (leaf 2.4%, flower 2.1%) relative to hexane (leaf 1.2%, flower 1.0%), dichloromethane (leaf 1.8%, flower 1.5%), and aqueous (leaf 2.9%, flower 2.5%). Qualitative phytochemical screening (Table 1) confirmed the presence of flavonoids, phenolics, tannins, saponins, terpenoids, steroids, and cardiac glycosides in both organs, with flavonoids and phenolics most abundant.

**Table 1:** Qualitative phytochemical screening of *Bauhinia monandra* leaf and flower extracts

| Phytochemical Constituent | Leaf Crude | Flower Crude | Leaf EAF | Flower EAF |
|---|---|---|---|---|
| Flavonoids | +++ | +++ | +++ | +++ |
| Phenolics | +++ | ++ | +++ | +++ |
| Tannins | ++ | + | ++ | ++ |
| Saponins | ++ | ++ | + | + |
| Alkaloids | + | + | + | + |
| Steroids/Terpenoids | ++ | + | + | + |
| Cardiac glycosides | + | + | + | + |
| Reducing sugars | + | + | - | - |

+++ = *abundant;* ++ = *moderate;* + = *trace;* - = *absent. EAF = ethyl acetate fraction.*

## 1. Total Phenolic and Flavonoid Contents

Total phenolic and flavonoid contents across all fractions are presented in Table 2 and illustrated in Figure 1. The ethyl acetate fraction consistently displayed the highest TPC (leaf: 121.5 +/- 3.2 mg GAE/g; flower: 109.8 +/- 2.9 mg GAE/g) and TFC (leaf: 63.7 +/- 2.1 mg QE/g; flower: 57.2 +/- 1.8 mg QE/g). The aqueous fraction ranked second in TPC but lower in TFC, reflecting hydrophilic tannins and phenolic acids. Non-polar fractions showed the lowest contents, consistent with their terpenoid and fatty-acid composition. Leaf fractions consistently exceeded corresponding flower fractions in both TPC and TFC across all polarity levels.

**Table 2:** Total phenolic content (TPC) and total flavonoid content (TFC) of *Bauhinia monandra* extracts and fractions (mean +/- SD, n=3)

| Fraction | TPC Leaf (mg GAE/g) | TPC Flower (mg GAE/g) | TFC Leaf (mg QE/g) | TFC Flower (mg QE/g) |
|---|---|---|---|---|
| Crude ethanol | 78.4 +/- 2.3 | 71.2 +/- 2.1 | 41.6 +/- 1.5 | 38.0 +/- 1.4 |
| n-Hexane | 12.1 +/- 0.8 | 10.5 +/- 0.6 | 6.2 +/- 0.4 | 5.1 +/- 0.3 |
| Dichloromethane | 34.7 +/- 1.2 | 30.2 +/- 1.1 | 18.4 +/- 0.9 | 15.9 +/- 0.8 |
| Ethyl acetate | 121.5 +/- 3.2* | 109.8 +/- 2.9* | 63.7 +/- 2.1* | 57.2 +/- 1.8* |
| Aqueous | 58.9 +/- 1.8 | 52.4 +/- 1.6 | 27.3 +/- 1.1 | 24.1 +/- 1.0 |

* Significantly different from all other fractions within the same organ ($p < 0.05$, Tukey's HSD).

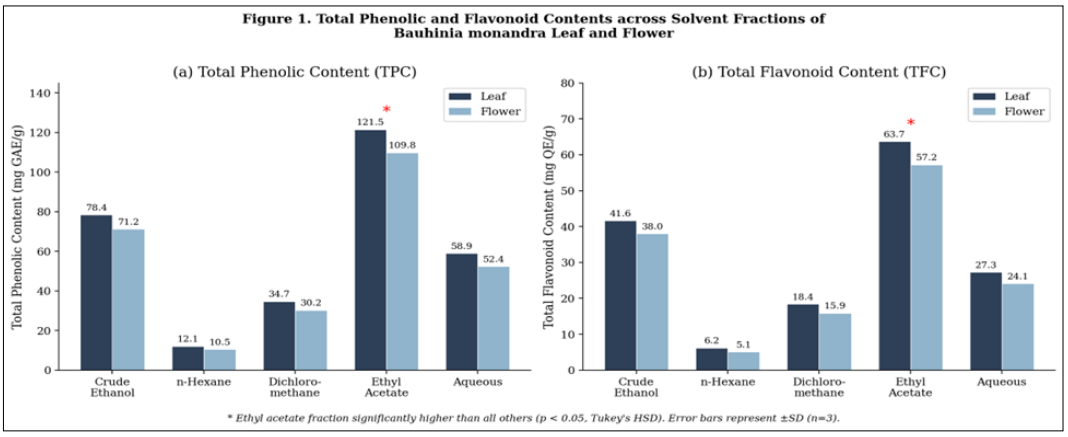


**Fig 1:** Total phenolic content (TPC, panel a) and total flavonoid content (TFC, panel b) across solvent fractions of *Bauhinia monandra* leaf and flower. The ethyl acetate fraction (EAF) exhibited significantly higher TPC and TFC than all other fractions in both organs (*$p < 0.05$). Error bars represent ±SD (n=3).

## 2. Alpha-Amylase Inhibitory Activity

All fractions inhibited alpha-amylase concentration-dependently across 31.25 to 1000 micrograms/mL. IC50 values (Table 3) showed a clear polarity-dependent pattern, illustrated in Figures 2 and 3. The ethyl acetate fractions showed the strongest inhibition (leaf IC50: 48.7 +/- 1.3 micrograms/mL; flower IC50: 61.2 +/- 1.7 micrograms/mL), followed by the crude ethanol extracts, aqueous fractions, dichloromethane, and n-hexane. Acarbose yielded IC50 of 23.5 +/- 0.8 micrograms/mL. One-way ANOVA confirmed significant differences among all fractions ($F = 287.4$, $p < 0.001$). Strong negative Pearson correlations were obtained between TPC and IC50 ($r = -0.936$, $p < 0.001$) and between TFC and IC50 ($r = -0.952$, $p < 0.001$; Figure 6), confirming phenolic and flavonoid content as the primary determinant of inhibitory potency.

**Table 3:** Alpha-amylase $IC_{o}50$ values of *Bauhinia monandra* extracts and fractions versus acarbose (mean +/- SD, n=3)

| Sample | IC50 Leaf (microg/mL) | IC50 Flower (microg/mL) | % Inhibition at 1000 microg/mL (Leaf/Flower) |
|---|---|---|---|
| Crude ethanol | 96.2 +/- 2.1 | 118.4 +/- 3.0 | 76.4 / 68.9 |
| n-Hexane | 612.5 +/- 8.4 | 690.1 +/- 9.1 | 34.2 / 29.8 |
| Dichloromethane | 210.3 +/- 4.6 | 248.7 +/- 5.2 | 61.5 / 55.1 |
| Ethyl acetate | 48.7 +/- 1.3* | 61.2 +/- 1.7* | 89.3 / 84.7 |
| Aqueous | 142.8 +/- 3.5 | 165.9 +/- 4.0 | 71.6 / 65.2 |
| Acarbose (standard) | 23.5 +/- 0.8 | 23.5 +/- 0.8 | 96.2 |

* Significantly different from all other fractions within the same organ ($p < 0.05$). Lower $IC_{50}$ = greater inhibitory potency.

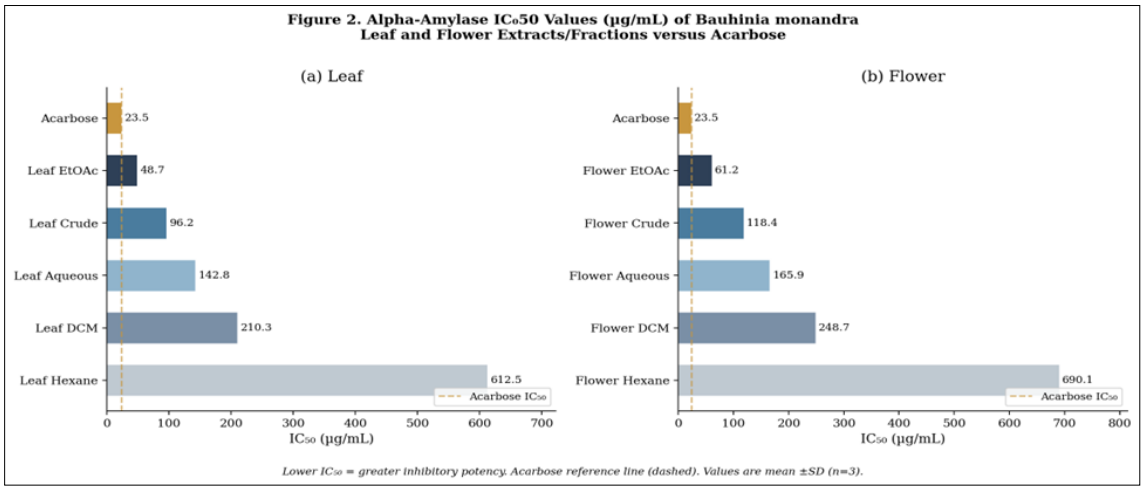


**Fig 2:** Alpha-amylase $IC_{50}$ values (µg/mL) for leaf (panel a) and flower (panel b) fractions of *Bauhinia monandra* compared to acarbose (dashed reference line). Lower $IC_{50}$ indicates greater potency. The ethyl acetate fraction (EAF) consistently achieves the strongest inhibition in both organs.

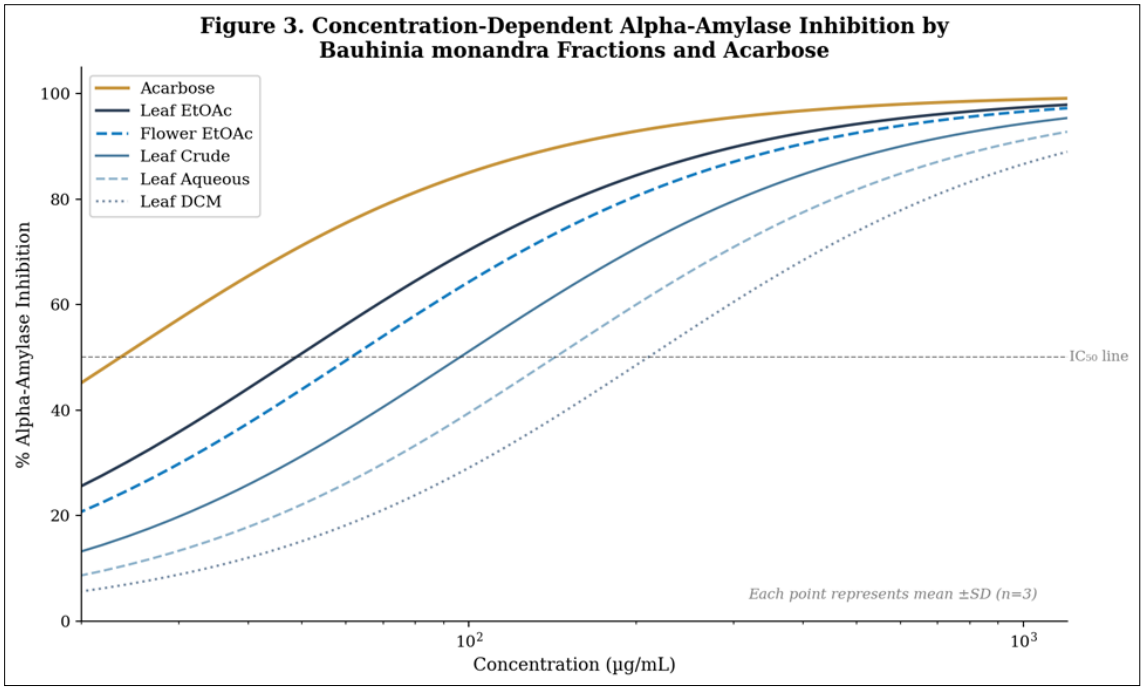


**Fig 3:** Concentration-dependent alpha-amylase inhibition (%) by *Bauhinia monandra* fractions and acarbose. Sigmoidal dose-response curves fitted by non-linear regression (GraphPad Prism 9). The 50% inhibition reference line is indicated. Log scale on x-axis.

## 3. LC-MS Characterisation of Polar Fractions

LC-MS analysis of the ethyl acetate and aqueous fractions identified six major compounds in the leaf (Table 4) and five in the flower. In both organs, quercetin-3-O-rutinoside (rutin; [M-H]- m/z 609.2) and quercetin ( [M-H]- m/z 301.1) were the dominant flavonoids, consistent with the earlier isolation reports of Aderogba *et al*. (2006) and Alade *et al*. (2012) [2, 4]. Kaempferol-3-O-rutinoside (m/z 593.2), quercetin-3-O-rhamnoside (quercitrin, m/z 447.1), and kaempferol (m/z 285.1) were also identified. Fragment ions at m/z 301 from rutin (loss of 308 Da, rutinose) and m/z 447 from kaempferol-3-O-rutinoside (loss of 146 Da, rhamnosyl) confirmed the identifications. Gallic acid (m/z 169.0) was detected in the aqueous fractions of both organs. The flower yielded a broadly similar phenolic profile to the leaf at lower peak intensities.

**Table 4:** LC-MS identified compounds from the ethyl acetate fraction of *Bauhinia monandra* leaf

| Peak | Compound | [M-H]- m/z | RT (min) | Fragment ions (m/z) | Fraction |
|---|---|---|---|---|---|
| 1 | Gallic acid | 169.0 | 4.2 | 125.0, 79.0 | EAF, AQF |
| 2 | Quercetin-3-O-rutinoside (Rutin) | 609.2 | 12.6 | 301.1, 255.0 | EAF |
| 3 | Quercetin-3-O-rhamnoside (Quercitrin) | 447.1 | 14.1 | 301.1, 179.0 | EAF |
| 4 | Kaempferol-3-O-rutinoside | 593.2 | 15.0 | 285.1, 447.1 | EAF |
| 5 | Quercetin | 301.1 | 18.3 | 179.0, 151.0 | EAF |
| 6 | Kaempferol | 285.1 | 20.1 | 163.0, 107.0 | EAF |

EAF = ethyl acetate fraction; AQF = aqueous fraction; RT = retention time; m/z values are monoisotopic; negative-ion ESI mode.

## 4. GC-MS Characterisation of Less-Polar Fractions

GC-MS analysis of the n-hexane and dichloromethane fractions identified seven major constituents (Table 5). Beta-sitosterol (RT 28.6 min, 11.5% area) and stigmasterol (RT 27.9 min, 7.2%) were the dominant phytosterols, consistent with Ferrari *et al*. (2019). Lupeol (RT 30.4 min, 4.0%), phytol (RT 19.5 min, 6.1%), squalene (RT 22.7 min, 4.8%), n-hexadecanoic acid (RT 18.2 min, 9.4%), and 9,12,15-octadecatrienoic acid (RT 19.9 min, 5.3%) were also identified. All identifications achieved NIST library match scores above 88% and Kovats retention index values within +/- 5 units of published standards.

The proportional distribution of compound classes is illustrated in Figure 4.

**Table 5:** GC-MS identified constituents from the n-hexane and dichloromethane fractions of *Bauhinia monandra* leaf

| Peak | Compound | RT (min) | % Area | KI Exp. | KI Lit. | Class |
|---|---|---|---|---|---|---|
| 1 | n-Hexadecanoic acid | 18.2 | 9.4 | 1964 | 1968 | Fatty acid |
| 2 | Phytol | 19.5 | 6.1 | 2117 | 2114 | Diterpene alcohol |
| 3 | 9,12,15-Octadecatrienoic acid | 19.9 | 5.3 | 2155 | 2152 | Fatty acid |
| 4 | Squalene | 22.7 | 4.8 | 2912 | 2908 | Triterpene |
| 5 | Stigmasterol | 27.9 | 7.2 | 3446 | 3441 | Phytosterol |
| 6 | Beta-sitosterol | 28.6 | 11.5 | 3498 | 3497 | Phytosterol |
| 7 | Lupeol | 30.4 | 4.0 | 3672 | 3669 | Triterpenoid |

KI Exp. = experimental Kovats retention index; KI Lit. = literature value; all match factors >=88%.

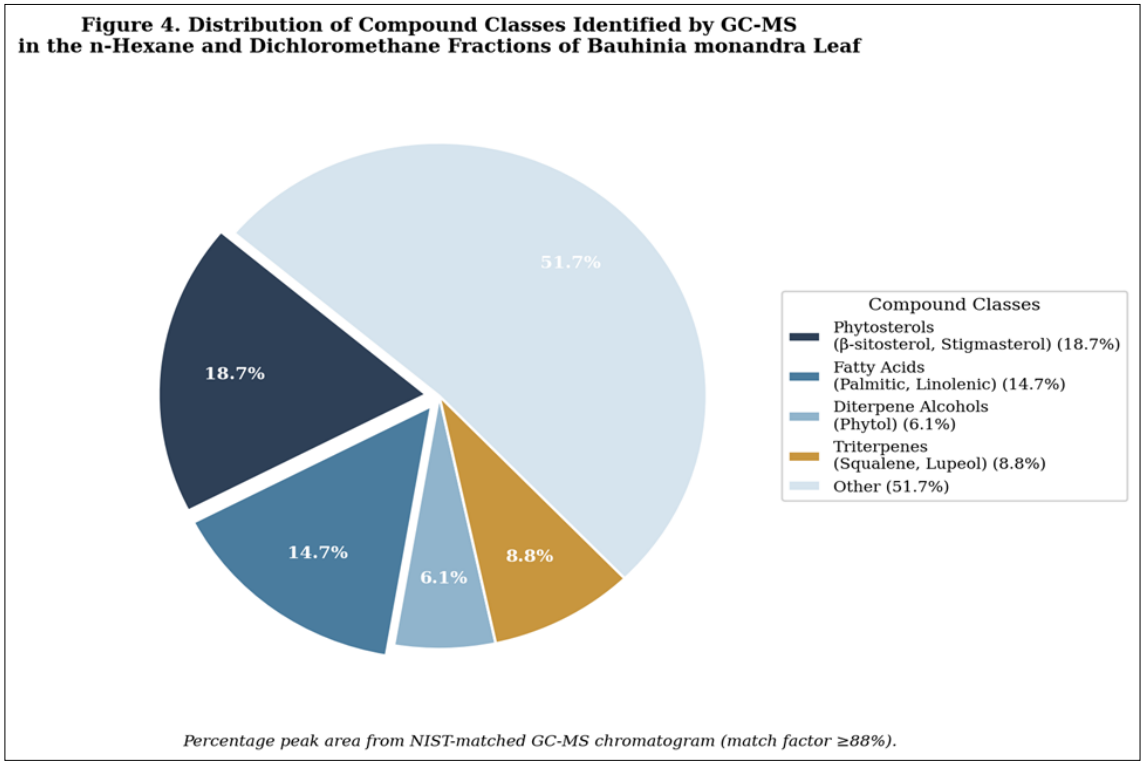


**Fig 4:** Distribution of chemical compound classes identified by GC-MS in the n-hexane and dichloromethane fractions of *Bauhinia monandra* leaf, expressed as percentage of total peak area. Phytosterols dominate, with fatty acids and diterpene alcohols as secondary constituents.

## 5. Molecular Docking Results

Acarbose redocking against PDB 1HNY yielded RMSD of 1.37 Angstrom, confirming protocol reliability. All docking results are presented in Table 6 and Figure 5. Among the flavonoids, rutin achieved the most favourable binding energy (-9.8 kcal/mol), forming hydrogen bonds with Asp197, Glu233, Asp300, Trp59, and Lys200. Quercetin (-8.6 kcal/mol) interacted with Asp197, Glu233, Asp300, and Gln63, consistent with its reported non-competitive inhibition (Shen *et al*., 2023). Kaempferol (-8.1 kcal/mol) engaged Asp300, Trp59, and Asp197. All three flavonoids outperformed acarbose (-7.5 kcal/mol).

In contrast, sterols (beta-sitosterol: -5.1 kcal/mol; stigmasterol: -5.3 kcal/mol) and lupeol (-5.8 kcal/mol) showed markedly weaker binding energies and lacked direct contacts with catalytic residues, interacting instead through hydrophobic contacts with peripheral residues (Val163, Leu165, Tyr151).

**Table 6:** AutoDock Vina binding energies and key interactions of identified compounds against pancreatic alpha-amylase (PDB: 1HNY)

| Compound | Binding Energy (kcal/mol) | Hydrogen Bond Interactions | Additional Interactions |
|---|---|---|---|
| **Rutin** | **-9.8** | Asp197, Glu233, Asp300, Trp59, Lys200 | pi-pi stacked: Trp59, Tyr62 |
| **Quercetin** | **-8.6** | Asp197, Glu233, Asp300, Gln63 | pi-pi T-shaped: Tyr62, Trp59 |
| Kaempferol | -8.1 | Asp300, Trp59, Asp197 | pi-pi stacked: Trp59; pi-OH: Tyr151 |

| | | | |
|---|---|---|---|
| Lupeol | -5.8 | None (no direct catalytic contacts) | pi-alkyl: Leu165, Val163, Tyr151 |
| Beta-sitosterol | -5.1 | None (no direct catalytic contacts) | Hydrophobic: Leu165, Pro163, Val163 |
| **Acarbose (reference)** | **-7.5** | Asp197, Glu233, Asp300, Gln63, Arg195 | H-bonds: Trp59, Tyr151, Lys200 |

Redocking validation RMSD = 1.37 Angstrom (PDB 1HNY). *Binding energies*: AutoDock Vina 1.2, exhaustiveness 8, grid box 30x30x30 Angstrom centred on Asp197/Glu233/Asp300. More negative = stronger predicted binding.

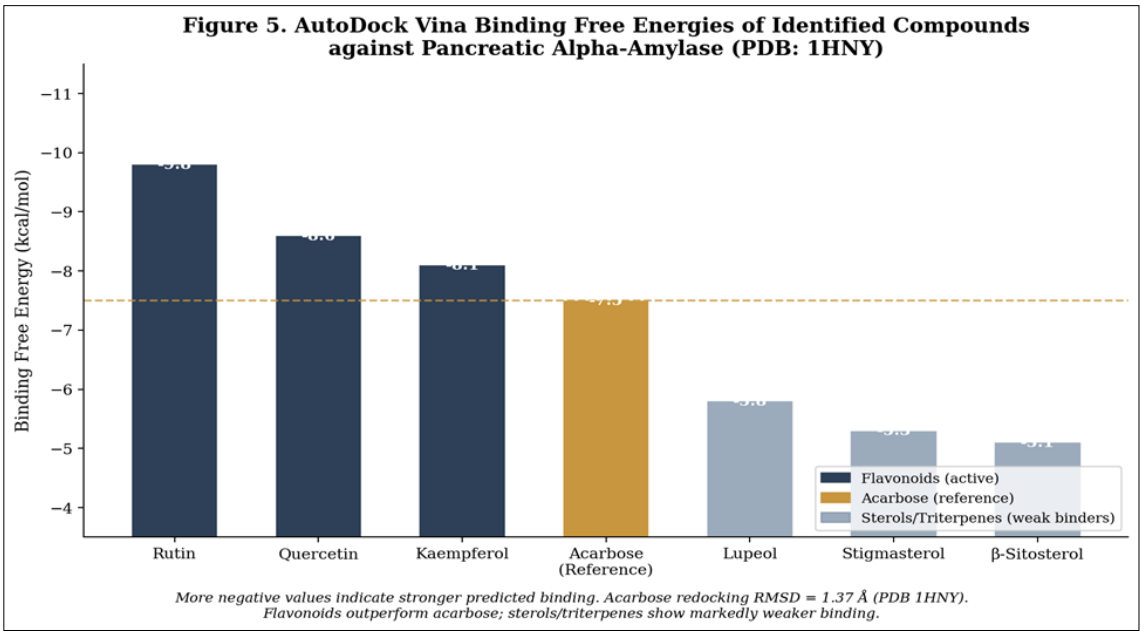


**Fig 5:** AutoDock Vina binding free energies (kcal/mol) of identified *Bauhinia monandra* compounds against pancreatic alpha-amylase (PDB: 1HNY). Flavonoids (rutin, quercetin, kaempferol) achieve binding energies more negative than the acarbose reference threshold (dashed line). Sterols and triterpenes bind peripherally without catalytic triad engagement.

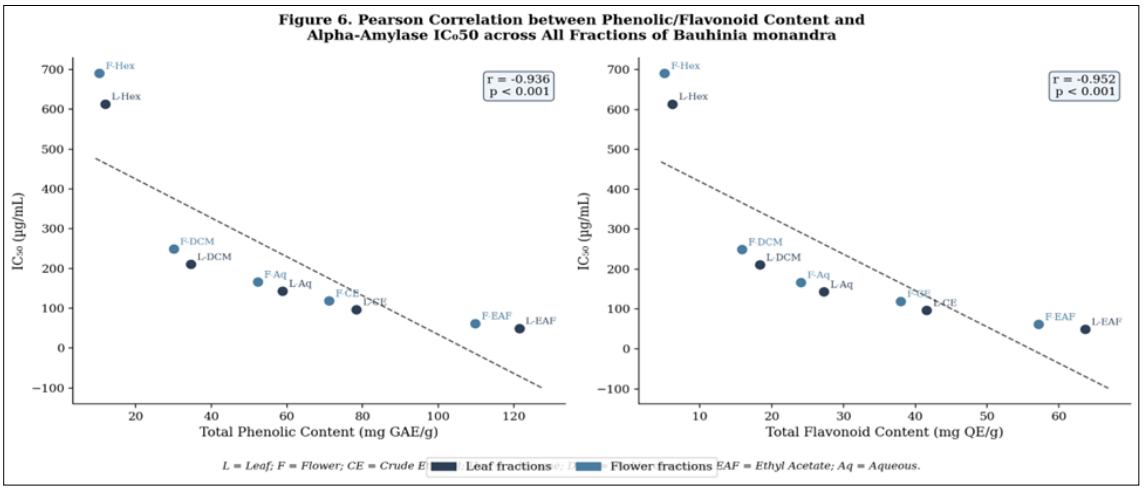


**Fig 6:** Pearson correlation between total phenolic content (TPC, panel a) and total flavonoid content (TFC, panel b) against alpha-amylase $IC_{50}$ across all fractions of *Bauhinia monandra* leaf and flower. Strong negative correlations (r = -0.936 and -0.952, $p < 0.001$) confirm phenolic/flavonoid content as the primary driver of inhibitory potency. L = Leaf; F = Flower; CE = Crude Ethanol; Hex = Hexane; DCM = Dichloromethane; EAF = Ethyl Acetate; Aq = Aqueous.

## Discussion

The results of this study assemble into a coherent and mechanistically consistent account of *B. monandra* as an alpha-amylase inhibitor, integrating polarity-guided partitioning, multi-platform chemical profiling, and computational target engagement for the first time. Four major interpretive threads run through the data.

First, the concentration of inhibitory activity in the ethyl acetate fraction, mirrored by the highest TPC and TFC in that same fraction (Figure 1, Table 2), reproduces a pattern documented consistently in Nigerian and African plant studies and reflects the preferential enrichment of flavonoid aglycones and glycosides in mid-polarity solvents. Adesegun *et al*. (2019) [3] reported the same TPC-TFC-IC50 trend for *Sorindea warneckei* and attributed it to ethyl acetate-concentrated quercetin, rutin, and gallic acid. Ojo *et al*. (2018) [21] demonstrated identical polarity patterning for *Mangifera indica* and *Spondias mombin* fractions. The strong Pearson correlations obtained in this study (TPC vs IC50: r = -0.936; TFC vs IC50: r = -0.952; Figure 6) confirm that phenolic and flavonoid content is the primary determinant of activity, rather than a non-specific extract effect or activity from the terpenoid-sterol pool concentrated in non-polar fractions.

Second, the chemical profiling is fully consistent with the established phytochemistry of the species. Aderogba *et al*.

(2006) [2] isolated quercetin-3-O-rutinoside and quercetin from the leaf; Alade *et al*. (2012) [4] confirmed these as the antihyperglycaemic principles; and Ferrari *et al*. (2019) [11] reported beta-sitosterol and a lupeol-type diol from the stem bark. The LC-MS detection of rutin (m/z 609), quercetin (m/z 301), quercitrin (m/z 447), kaempferol-3-O-rutinoside (m/z 593), and kaempferol (m/z 285) in the polar fractions of both leaf and flower (Table 4) extends this known chemical fingerprint to the flower for the first time and provides a foundation for its therapeutic use. The GC-MS detection of beta-sitosterol (11.5% area), stigmasterol, and lupeol in non-polar fractions (Table 5, Figure 4) complements the stem-bark phytochemistry, establishing chemical continuity across plant organs.

Third, molecular docking provides a structural rationale bridging the *in vitro* and phytochemical observations. All three identified flavonols (rutin: -9.8 kcal/mol; quercetin: -8.6 kcal/mol; kaempferol: -8.1 kcal/mol) achieved binding energies superior to acarbose (-7.5 kcal/mol; Figure 5, Table 6), with hydrogen bonds formed directly with the catalytic triad residues Asp197, Glu233, and Asp300. This corroborates the literature-reported non-competitive and competitive inhibition kinetics of quercetin (IC50 0.325 mg/mL versus acarbose 0.622 mg/mL; Shen *et al*., 2023) [28] and the highly favourable rutin binding reported against porcine alpha-amylase (Kulkarni and Kamble, 2021) [16]. The structure-activity relationship principle established by Martinez-Gonzalez *et al*. (2019) [17] that C3 and C4 hydroxylation of the B-ring, combined with a C2-C3 double bond and C4 carbonyl, are the primary structural determinants of flavonol potency is wholly supported by the ranking quercetin > kaempferol observed here, since quercetin carries an additional B-ring hydroxyl absent in kaempferol. Conversely, the weak binding of beta-sitosterol (-5.1 kcal/mol) and lupeol (-5.8 kcal/mol), which lacked direct contacts with the catalytic triad, confirms that sterols and triterpenoids in the non-polar fractions are unlikely primary enzyme inhibitors, consistent with the low alpha-amylase inhibition in the hexane and dichloromethane fractions (Figure 2).

Fourth, the present mechanistic findings contextualise existing *in vivo* antidiabetic evidence. Alade *et al*. (2011) [5] demonstrated 65 percent blood glucose reduction at 2 g/kg in alloxan-diabetic rats, and Menezes *et al*. (2007) [18] documented comparative antidiabetic activity of *B. monandra* in Brazilian populations. The present study offers the molecular entry point those *in vivo* studies lacked, proposing alpha-amylase inhibition mediated by rutin and quercetin engaging the catalytic triad as a contributing mechanism to the hypoglycaemic effect. Benchmarking against comparable studies is instructive: the leaf ethyl acetate IC50 of 48.7 micrograms/mL compares favourably with *Sorindea warneckei* (400 micrograms/mL; Adesegun *et al*., 2019) [3] and most Nigerian crude-extract comparators, though it falls above the exceptional potency of *Macaranga barteri* (IC50 0.54 micrograms/mL, approaching acarbose 0.68 micrograms/mL; Discover Plants, 2025), representing a moderately strong inhibitor suitable for further bioassay-guided isolation.

Two methodological caveats must be noted. The DNSA assay overestimates IC50 relative to chromogenic methods; acarbose is partially thermolabile under boiling-water-bath conditions (Visvanathan and Williamson, 2023) [33], meaning absolute potency comparisons across laboratories are unreliable and inter-study IC50 values should be treated as indicative. AutoDock Vina binding energies are protocol- and receptor-structure-dependent and represent predicted relative binding rather than actual dissociation constants. These limitations define the next experimental steps rather than invalidate the current conclusions.

## Conclusion

This study furnishes the first integrated phytochemical and mechanistic account of *Bauhinia monandra* as a pancreatic alpha-amylase inhibitor, spanning both leaf and flower organs and combining *in vitro* bioassay, LC-MS and GC-MS chemical profiling, and computational docking. Inhibitory activity concentrates in the flavonoid- and phenolic-rich ethyl acetate fractions, with the leaf ethyl acetate fraction achieving an IC50 of 48.7 micrograms/mL. LC-MS analysis established rutin, quercetin, quercitrin, and kaempferol derivatives as major polar constituents, while GC-MS identified beta-sitosterol, stigmasterol, and lupeol in the non-polar fractions. Molecular docking positioned rutin (-9.8 kcal/mol), quercetin (-8.6 kcal/mol), and kaempferol (-8.1 kcal/mol) within the catalytic triad of alpha-amylase, all outperforming acarbose (-7.5 kcal/mol). Together with prior *in vivo* hypoglycaemic evidence, these data provide a defensible mechanistic rationale for the traditional antidiabetic use of *B. monandra* and validate the flower as a previously neglected, pharmacologically credible source of carbohydrase inhibitors. Future priorities include bioassay-guided isolation of pure active flavonoids, enzyme kinetic analysis (mode of inhibition), chromogenic assay cross-validation, and molecular dynamics simulation of the rutin-alpha-amylase complex, as the prioritised steps toward a standardised antidiabetic phytomedicine.

## Declarations


### Funding

This research received no specific grant from any funding agency in the public, commercial, or not-for-profit sectors.


### Ethical Statement

*Bauhinia monandra* is a widely cultivated ornamental plant. No human subjects or vertebrate animals were used in this study; no further ethical clearance beyond standard laboratory-chemical safety protocols was required.

## References


1. Abo KA, Jimoh FO. Antihyperglycemic potential of stem bark of *Bauhinia monandra* Kurz in rats. Nigerian Journal of Natural Products and Medicine,2004:8:48-51.
2. Aderogba MA, Ogundaini AO, Eloff JN. Isolation of two flavonoids from *Bauhinia monandra* (Kurz) leaves and their antioxidative effects. African Journal of Traditional, Complementary and Alternative Medicines,2006:3(4):59-65. https://doi.org/10.4314/ajtcam.v3i4.31177
3. Adesegun SA, Badejo MV, Odebunmi SO, Ojobo PD, Coker HB. Alpha amylase inhibitory and antioxidant activities of leaf extract and fractions of *Sorindea warneckei* Engl. (Anacardiaceae). Tropical Journal of Natural Product Research, 2019, 3(2). https://doi.org/10.26538/tjnpr/v3i2.7

4. Alade GO, Adebajo AC, Omobuwajo OR, Proksch P, Verspohl EJ. Quercetin, a minor constituent of the antihyperglycemic fraction of *Bauhinia monandra* leaf. Journal of Diabetes,2012:4(4):439-441. https://doi.org/10.1111/j.1753-0407.2012.00222.x
5. Alade GO, Omobuwajo OR, Alade TO, Adebajo AC, Proksch P, Verspohl EJ. Evaluation of the hypoglycaemic activity of *Bauhinia monandra* leaf in alloxan-diabetic rats and INS-1 insulin cells. Journal of Chemical and Pharmaceutical Research,2011:3:563-571.
6. Argolo ACC, Sant'Ana AEG, Pletsch M, Coelho LCBB. Antioxidant activity of leaf extracts from *Bauhinia monandra*. Bioresource Technology,2004:95(2):229-233. https://doi.org/10.1016/j.biortech.2003.12.014
7. Brayer GD, Luo Y, Withers SG. The structure of human pancreatic alpha-amylase at 1.8 Angstrom resolution and comparisons with related enzymes. Protein Science,1995:4(9):1730-1742. https://doi.org/10.1002/pro.5560040908
8. Brayer GD, Sidhu G, Maurus R, Rydberg EH, Braun C, Wang Y, *et al*. Subsite mapping of the human pancreatic alpha-amylase active site through structural, kinetic, and mutagenesis techniques. Biochemistry,2000:39(16):4778-4791. https://doi.org/10.1021/bi9921182
9. Campos JKL, Araujo CSF, Araujo TFS, Santos AFS, Teixeira JA, Lima VLM, *et al*. Anti-inflammatory and antinociceptive activities of *Bauhinia monandra* leaf lectin. Biochimie Open,2016:2:62-68. https://doi.org/10.1016/j.biopen.2016.02.003
10. Cechinel-Filho V. Chemical composition and biological potential of plants from the genus *Bauhinia*. Phytotherapy Research,2009:23(10):1347-1354. https://doi.org/10.1002/ptr.2756
11. Ferrari J, de Oliveira DM, Aragao NM. Phytochemical constituents isolated from the stem bark of *Bauhinia monandra*. Floresta e Ambiente,2019:26(1):e20150285. https://doi.org/10.1590/2179-8087.150285
12. Galicia-Garcia U, Benito-Vicente A, Jebari S, Larrea-Sebal A, Siddiqi H, Uribe KB, *et al*. Pathophysiology of type 2 diabetes mellitus. International Journal of Molecular Sciences,2020:21(17):6275. https://doi.org/10.3390/ijms21176275
13. Haruna A, Yahaya SM. Recent advances in the chemistry of bioactive compounds from plants and soil microbes: a review. Chemistry Africa,2021:4(2):231-248. https://doi.org/10.1007/s42250-021-00215-1
14. International Diabetes Federation. Type 2 diabetes. Retrieved from https://idf.org/about-diabetes/types-of-diabetes/type-2/, 2021.
15. Kerru N, Singh-Pillay A, Awolade P, Singh P. Current anti-diabetic agents and their molecular targets: a review. European Journal of Medicinal Chemistry,2018:152:436-488. https://doi.org/10.1016/j.ejmech.2018.04.061
16. Kulkarni AA, Kamble AD. Flavonoids from *Argyreia nervosa* as potential alpha-amylase inhibitors. Biology and Life Sciences Forum,2021:4(1):56. https://doi.org/10.3390/IECPS2020-08773
17. Martinez-Gonzalez AI, Diaz-Sanchez AG, de la Rosa LA, Bustos-Jaimes I, Alvarez-Parrilla E. Evaluation of a flavonoids library for inhibition of pancreatic alpha-amylase towards a structure-activity relationship. Journal of Enzyme Inhibition and Medicinal Chemistry,2019:34(1):1-10. https://doi.org/10.1080/14756366.2018.1545767
18. Menezes FS, Minto ABM, Ruela HS, Kuster RM, Sheridan H, Frankish N. Hypoglycemic activity of two Brazilian *Bauhinia* species: *Bauhinia forficata* L. and *Bauhinia monandra* Kurz. Revista Brasileira de Farmacognosia,2007:17(1):8-13. https://doi.org/10.1590/S0102-695X2007000100003
19. Molecules. Flavonoid in all their therapeutic values: an odyssey into the phytochemistry and pharmacology of naturally occurring flavonoid from genus *Bauhinia*. Molecules,2025:30(16):3335. https://doi.org/10.3390/molecules30163335
20. Ogboye RM, Patil RB, Famuyiwa SO, Faloye KO. Novel alpha-amylase and alpha-glucosidase inhibitors from selected Nigerian antidiabetic plants: an in silico approach. Journal of Biomolecular Structure and Dynamics, 2021, 1-10. https://doi.org/10.1080/07391102.2021.1918237
21. Ojo OA, Afon AA, Ojo AB, Ajiboye BO, Oyinloye BE, Kappo AP. Inhibitory effects of solvent-partitioned fractions of two Nigerian herbs (*Spondias mombin* Linn. and *Mangifera indica* L.) on alpha-amylase and alpha-glucosidase. Antioxidants,2018:7(6):73. https://doi.org/10.3390/antiox7060073
22. Olamoyegun MA, Olamoyegun AD, Abiodun AA, Fasanmade OA. A systematic review and meta-analysis of the prevalence and risk factors of type 2 diabetes mellitus in Nigeria. Clinical Diabetes and Endocrinology,2024:10(1):43. https://doi.org/10.1186/s40842-024-00209-1
23. Olaokun OO, Zubair MS. Antidiabetic activity, molecular docking, and ADMET properties of compounds isolated from bioactive ethyl acetate fraction of *Ficus lutea* leaf extract. Molecules,2023:28(23):7717. https://doi.org/10.3390/molecules28237717
24. Oshingboye AD. Molecular characterization and DNA barcoding of arid-land species of family Fabaceae in Nigeria (Doctoral dissertation, University of Lagos, Nigeria), 2017.
25. Proenca C, Ribeiro D, Freitas M, Fernandes E. Flavonoids as potential agents in the management of type 2 diabetes through the modulation of alpha-amylase and alpha-glucosidase activity: a review. Critical Reviews in Food Science and Nutrition,2022:62(12):3137-3207. https://doi.org/10.1080/10408398.2020.1862755
26. Quazi A, Makeshwar BH, Patil PH, Desai PM. *In vitro* alpha-amylase enzyme assay of hydroalcoholic polyherbal extract. Evidence-Based Complementary and Alternative Medicine, 2022, 1577957. https://doi.org/10.1155/2022/1577957
27. Saeedi P, Salpea P, Karuranga S, Petersohn I, Malanda B, Gregg EW, *et al*. Mortality attributable to diabetes in 20-79 years old adults, 2019 estimates: Results from the IDF Diabetes Atlas, 9th edition. Diabetes Research and

Clinical Practice,2020:162:108086. https://doi.org/10.1016/j.diabres.2020.108086
28. Shen H, Xu H, Wang Q, Zheng Y, Su Y. Structure-activity relationships and the underlying mechanism of alpha-amylase inhibition by hyperoside and quercetin. Spectrochimica Acta Part A,2023:285:122105. https://doi.org/10.1016/j.saa.2022.122105
29. Sun H, Saeedi P, Karuranga S, Pinkepank M, Ogurtsova K, Duncan BB, *et al*. IDF Diabetes Atlas: global, regional and country-level diabetes prevalence estimates for 2021 and projections for 2045. Diabetes Research and Clinical Practice,2022:183:109119. https://doi.org/10.1016/j.diabres.2021.109119
30. Trott O, Olson AJ. AutoDock Vina: improving the speed and accuracy of docking with a new scoring function, efficient optimization, and multithreading. Journal of Computational Chemistry,2010:31(2):455-461. https://doi.org/10.1002/jcc.21334
31. Uloko AE, Musa BM, Ramalan MA, Gezawa ID, Puepet FH, Uloko AT, *et al*. Prevalence and risk factors for diabetes mellitus in Nigeria: a systematic review and meta-analysis. Diabetes Therapy,2018:9(3):1307-1316. https://doi.org/10.1007/s13300-018-0441-1
32. Velu G, Palanichamy V, Rajan AP. Phytochemical and pharmacological importance of plant secondary metabolites in modern medicine. Bioorganic Phase in Natural Food: An Overview, 2018, 135-156.
33. Visvanathan R, Williamson G. Chromogenic assay is more efficient in identifying alpha-amylase inhibitory properties of anthocyanin-rich samples when compared to the DNSA assay. Molecules,2023:28(17):6399. https://doi.org/10.3390/molecules28176399
34. World Health Organization. Diabetes fact sheet. Geneva: WHO. Retrieved from https://www.who.int/news-room/fact-sheets/detail/diabetes, 2021.
35. Ye Q, Song X, Li C, Wang X, Zhang J. Ionic liquid-based microwave-assisted extraction of flavonoids from *Bauhinia championii* (Benth.) Benth. Molecules,2012:17(12):14323-14335. https://doi.org/10.3390/molecules171214323